Wind-Tunnel and Flight Tests of a Delta-Wing Remotely Piloted Vehicle

Long P. Yip,* David J. Fratello,† and David B. Robelen‡
NASA Langley Research Center, Hampton, Virginia 23665
and
George M. Makowiec§
Vigyan Research Associates, Inc., Hampton, Virginia 23666

At the request of the United States Marine Corps, an exploratory wind-tunnel and flight-test investigation was conducted by NASA Langley Research Center on the Marine Corps' Exdrone remotely piloted vehicle configuration. Static wind-tunnel tests were conducted to identify and improve the stability and control characteristics of the vehicle. The wind-tunnel tests resulted in several configuration modifications, including increased elevator area, increased vertical tail area and moment arm, increased rudder area and aileron area, the addition of vertical wingtip fins, and the addition of leading-edge droops on the outboard wing panel to improve stall departure resistance. Flight tests showed improved flight characteristics of the modified configuration.

Nomenclature

b	=	wing span, ft
C_L	=	lift coefficient, lift/qS
C_l	=	rolling-moment coefficient, rolling moment/qSb
$C_{l\beta}$	=	rolling-moment coefficient due to sideslip, /deg
C_m	=	pitching-moment coefficient, pitching moment/qSc_{ref}
C_n	=	yawing-moment coefficient, yawing moment/qSb
$C_{n\beta}$	=	yawing-moment coefficient due to sideslip, /deg
$C_{n\beta,\text{dyn}}$	=	dynamic directional stability parameter, $C_{n\beta}\cos\alpha-(I_Z/I_X)C_{l\beta}\sin\alpha$
C_T	=	thrust coefficient, T/qS
C_Y	=	side-force coefficient, side force/qS
$C_{Y\beta}$	=	side-force coefficient due to sideslip, /deg
c_{ref}	=	reference wing chord (theoretical root chord used), 4.458 ft
I_X, I_Z	=	mass moment of inertia about X and Z axes, respectively, slug-ft^2
q	=	freestream dynamic pressure, psf
S	=	reference wing area, 21.24 ft^2
T	=	effective thrust, drag (propeller removed) − drag (propeller operating)
α	=	angle of attack, deg
β	=	angle of sideslip, deg
ΔC_l	=	incremental rolling-moment coefficient
ΔC_n	=	incremental yawing-moment coefficient
ΔC_Y	=	incremental side-force coefficient
δ_a	=	aileron deflection per side, positive trailing-edge down, deg
δ_e	=	elevator deflection, positive trailing-edge down, deg
δ_r	=	rudder deflection, positive trailing-edge left, deg

Subscripts

l	=	left
r	=	right

Introduction

IN recent years, there has been keen interest in the military to develop remotely piloted, unmanned flight vehicles. The Exdrone RPV (remotely piloted vehicle) configuration is a low-

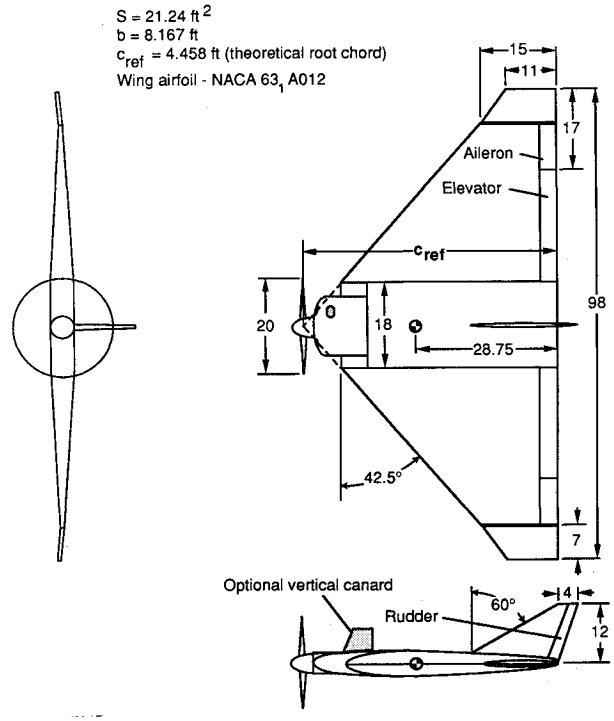

Fig. 1 Three-view sketch of baseline configuration.

Presented as Paper 90-1261 at the AIAA/SFTE/DGLR/SETP 5th Biannual Flight Test Conference, Ontario, CA, May 21-24, 1990; received June 14, 1990; revision received Jan. 28, 1991; accepted for publication April 6, 1991.

*Research Engineer, Flight Research Branch, Flight Applications Division. Senior Member AIAA
†Research Engineer, Flight Dynamics Branch, Flight Applications Division.
‡Engineering Technician, Operations Support Division.
§Engineering Technician, 30 Research Drive.

cost unmanned flight vehicle being developed by the United States Marine Corps to provide support capabilities in various mission roles. The Exdrone RPV is basically a delta-wing configuration powered by a tractor propeller propulsion system. In preliminary flight tests conducted by the Marine Corps, the vehicle exhibited weak stability and control characteristics in low-speed flight and a tendency to depart in the lateral-directional axes near the stall. At the request of the Marine Corps, an exploratory wind-tunnel and flight-test investigation was conducted by the NASA Langley Research Center to improve the stability and control and general flight characteristics of the Exdrone configuration.

To accomplish this objective, exploratory wind-tunnel and flight tests were conducted to determine the configuration's basic aerodynamic characteristics, to identify problem areas, and to provide modifications for aerodynamic improvements. As a result of the wind-tunnel study, the Marine Corps incorporated the modifications into the Exdrone design. Flight tests were conducted at the NASA Plum Tree Test Site to provide a qualitative evaluation of the flight characteristics of the modified configuration. The results of the wind tunnel and flight tests are reported herein.

Remotely Piloted Vehicle Configuration Description

Two configurations of the Exdrone RPV were tested in a low-speed wind tunnel with a 12-ft octagonal test section. A three-view sketch of the baseline configuration is shown in Fig. 1. The second configuration, which was modified according to recommendations from the initial wind-tunnel test, was also tested in the wind tunnel. A three-view sketch of the modified configuration is presented in Fig. 2. The modifications included increased elevator area, increased vertical tail area and moment arm, and increased rudder area and aileron area. The aileron deflection schedule was modified to provide unequal, differential motion with more up deflection than down in order to minimize adverse yaw characteristics. Vertical wingtip fins were added to improve directional stability, and a leading-edge droop was added to the outboard wing panel to improve stall departure resistance. The leading-edge droop modification was applied to the wingtip extension from the wingtip/fin juncture to the tip. The wingtip fin

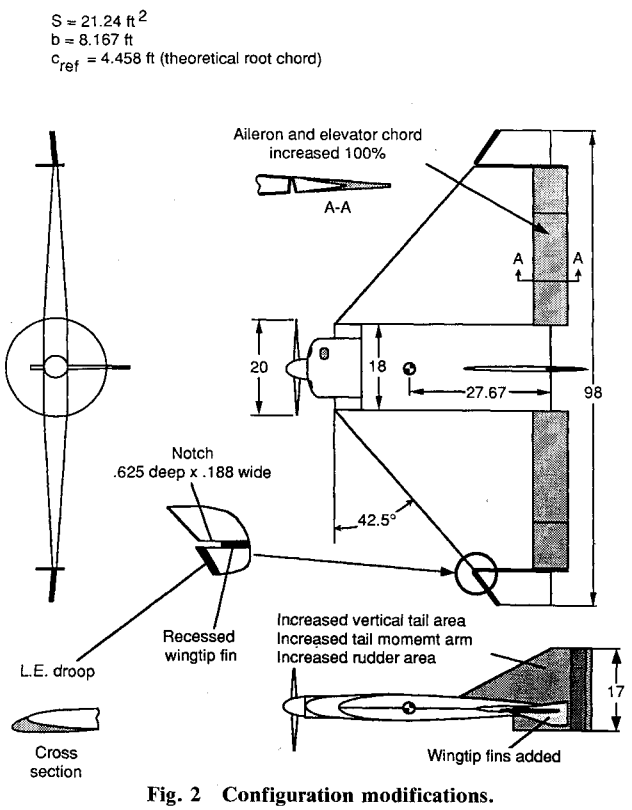

Fig. 2 Configuration modifications.

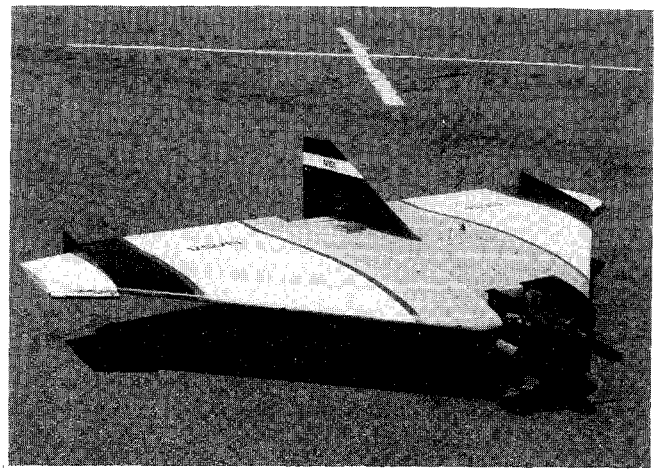

Fig. 3 Modified configuration at the NASA Plum Tree Test Site.

was recessed 0.625 in. to provide for a small notch (see Fig. 2). The notch was added to enhance the vortex flow from the snag inboard edge of the leading-edge droop to keep the flow attached on the wingtip panel at high angles of attack (see Ref. 1). Past studies have shown that the improved flow characteristics of the outer wing panel provided increased roll damping in the stall and poststall angle-of-attack range (see Refs. 2–5).

Wind-Tunnel Tests

The static wind-tunnel tests were conducted in the Langley 12-ft low-speed tunnel. Tests were conducted at a freestream dynamic pressure of 4 psf, which corresponds to a Reynolds number of approximately 1.67×10^6 based on the reference chord. This tunnel condition approximated actual flight conditions near the stall. The angle-of-attack range of the tests was from 0 to 30 deg, and the angle-of-sideslip range was from -16 to 16 deg. For this investigation, tunnel corrections were not considered necessary because of the emphasis in investigating the high angle-of-attack stability and control characteristics.

For the wind tunnel tests, the fuselage was structurally modified to accommodate a six-component strain-gauge balance for measuring aerodynamic forces and moments. All longitudinal forces and moments are referred to the wind axis system, and all lateral-directional forces and moments are referred to the body axis system. Power-on tests were conducted using a turbine air motor to supply power to the propeller. A commercially available propeller 20 in. in diameter with a 14-in. pitch was used. Values of C_T from 0 to 0.75 were obtained in the wind tunnel by lowering the freestream dynamic pressure. For the condition of $C_T = 0$, the propeller was not installed on the model. The reference moment center was located at 46.3% of c_{ref} for the baseline configuration (see Fig. 1). For the modified model, the reference moment center was moved aft to a location of 48.3% of c_{ref} (see Fig. 2).

Flight-Test Setup

Qualitative flight-test evaluations were performed at the NASA Plum Tree Test Site on the modified configuration to confirm the effect of modification improvements on stability, controllability, and general flight behavior. A photograph of the modified Exdrone at the Plum Tree Test Site is shown in Fig. 3. A description of the Plum Tree Test Site is given in Ref. 6. The Exdrone RPV was equipped with a radio-controlled flight system that included an onboard receiver, control servos, and batteries for electrical power. The command control transmitter allowed the rudder inputs to be integrated with the aileron inputs. A rudder-to-aileron interconnect could be switched on to allow the rudder to command turning flights with shallow bank angles. A rate gyro was used to augment the roll damping of the configuration.

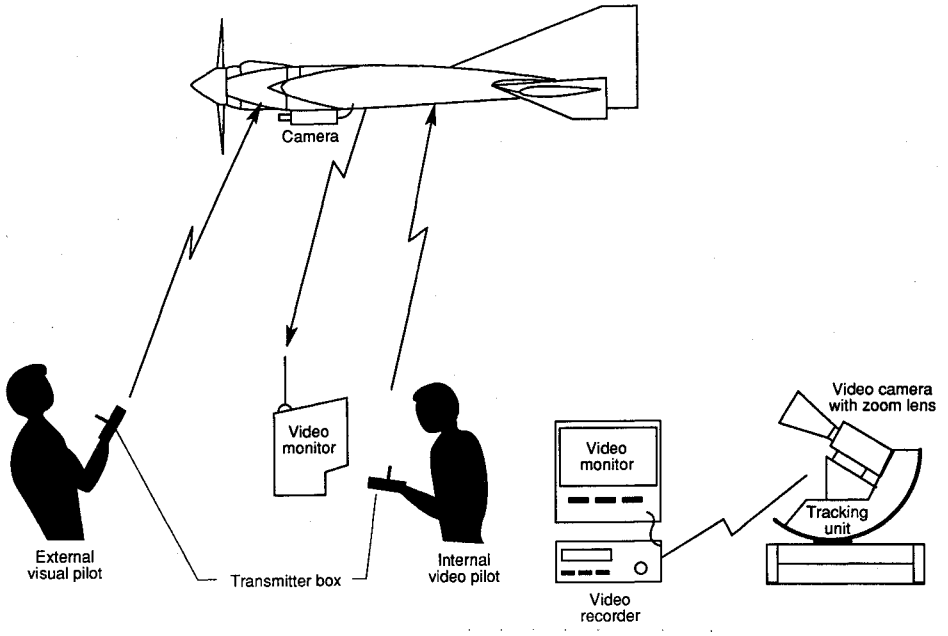

Fig. 4 Illustration of flight-test setup.

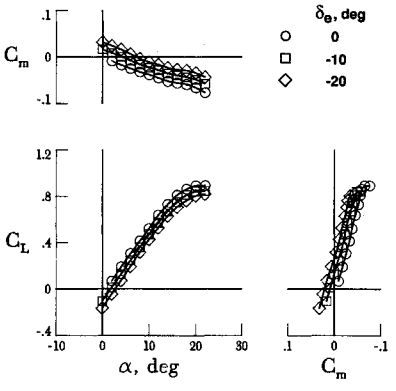

Fig. 5 Effect of elevator deflection on the longitudinal aerodynamic characteristics of the baseline configuration.

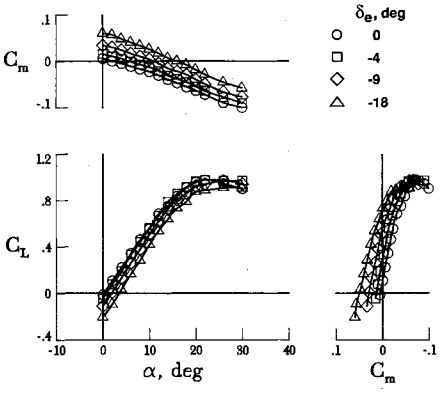

Fig. 6 Effect of elevator deflection on the modified configuration.

Power for the vehicle was provided by a modified, two-stroke chain-saw engine, which developed about 6.6 hp from a 5.8-in.^{3} displacement. The propeller had a 20-in. diam and a 14-in. pitch and was located in a tractor position on the RPV. The vehicle weighed 35 lb empty and was designed to carry 26 lb of payload with 4 lb of fuel for a nominal maximum takeoff gross weight of 65 lb.

The vehicle was launched on a takeoff dolly by stretching bungee chords a distance of approximately 80–90 ft to assist in acceleration of the vehicle during takeoff. For recovery, a front skid pad and rear skid wires were attached on the underside of the vehicle.

The basic flight-test setup is illustrated in Fig. 4. The vehicle was flown remotely by either an outdoor visual pilot or an indoor video pilot. An onboard video camera was used to transmit a forward view from the onboard camera system to the ground-based video pilot. A ground-based tracking camera was used to follow the motions of each flight maneuver.

Flight Evaluation Procedure

The configuration's flight characteristics were evaluated using the following flight maneuvers.

1) The vehicle was flown with wings level and power reduced to idle at the start of the maneuver. The control stick was gradually pulled to a full-back position and held at that position with inputs of aileron and rudder to maintain heading. After stabilizing the vehicle, the throttle was then gradually increased until full power was applied to determine the effects of power at high-angle-of-attack flight conditions.

2) With the vehicle trimmed in level flight, rapid elevator or rudder inputs were used to excite the configuration for either longitudinal or lateral-directional motions. For each evaluation, the control surface was deflected from full negative to full positive values to perturb the vehicle's motions about a particular axis. The control stick was then quickly released to the previously determined trimmed settings, and the vehicle's damping characteristics were evaluated by observing its motions following the doublet inputs.

Wind-Tunnel Test Results

Longitudinal aerodynamic characteristics are shown in Figs. 5–9. Figure 5 shows the lift and pitching-moment characteristics of the baseline configuration with elevator deflections of 0, 10, and 20 deg trailing-edge up. The data indicate linear lift and pitching-moment variations for angle-of-attack values up to about 12 deg. Above an angle of attack of 12 deg, the configuration exhibited nonlinear aerodynamic characteristics, which were probably caused by the development of spanwise flow typically associated with the swept wing platform. The longitudinal stability of the baseline configuration was positive throughout the test angle-of-attack range. For the baseline configuration at its nominal center-of-gravity location, the

longitudinal static margin was about 6% based on the reference chord. The maximum nose-up pitch control for the baseline configuration (20 deg trailing-edge up elevator deflection) provided a maximum trimmed angle of attack of about 7 deg, which corresponds to a maximum trimmed lift coefficient of about $C_L = 0.25$.

To increase the pitch trim capability of the vehicle, several configuration changes were considered. These included relaxing the longitudinal stability, increasing the elevator deflection, and increasing elevator area. Because the vehicle was constrained to a limited c.g. envelope from payload considerations and because of the need to keep the control system simple, relaxing the longitudinal static stability was not acceptable as a means for achieving higher trim angles of attack. Also, deflecting the elevator to a higher setting would have caused flow separation and put the elevator control surface in a nonlinear angle range. A chord extension to the elevator control surface was used to increase nose-up trim capability.

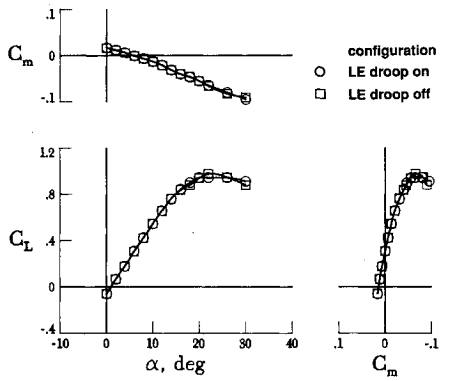

Fig. 7 Effect of leading-edge droop modification on the longitudinal aerodynamic characteristics on the modified configuration.

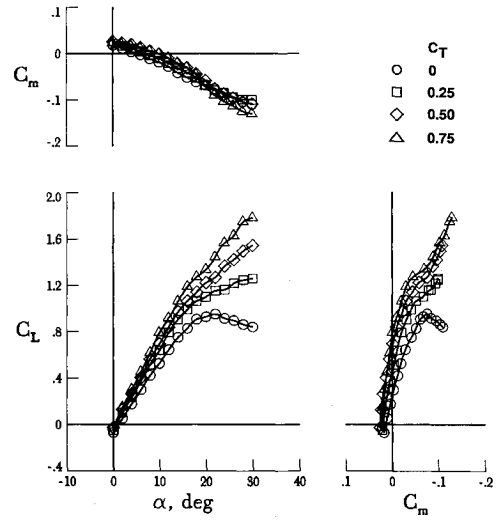

Fig. 8 Effect of power on the longitudinal aerodynamic characteristics, modified configuration.

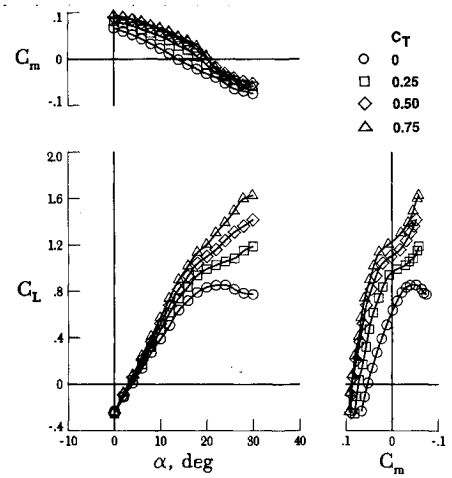

Fig. 9 Effect of power on the longitudinal aerodynamic characteristics, modified configuration with maximum nose-up control.

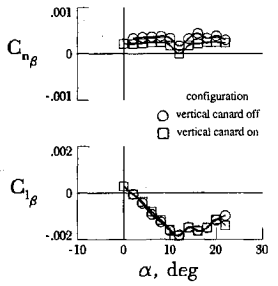

Fig. 10 Lateral-directional stability of the baseline configuration.

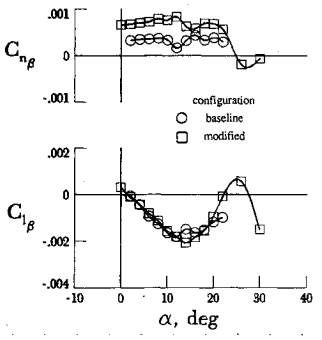

Fig. 11 Comparison of lateral-directional stability characteristics between baseline and modified configurations.

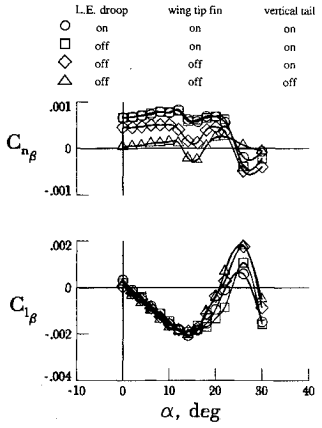

Fig. 12 Effect of various configuration components on the lateral-directional stability characteristics, modified configuration.

The modified Exdrone configuration incorporated the larger elevator chord and was wind-tunnel tested with the moment reference center at 2.5% of the reference chord aft of the baseline configuration. The ailerons were rigged symmetrically 4 deg sailing-edge up to provide additional nose-up moments for pitch trim. The longitudinal aerodynamic characteristics of the modified configuration for various elevator deflections are shown in Fig. 6. The data indicate stable pitching-moment characteristics for the test angle-of-attack range. Maximum trimmed angle of attack for the modified configuration was about 15 deg, which resulted in a trimmed lift coefficient of about 0.7. In terms of minimum level flight speeds, the increase in trimmed lift, for the nominal vehicle gross weight of 65 lb, reduced the minimum flight speed from 69 mph for the baseline configuration to 41 mph for the modified configuration.

The effect of the leading-edge droop modification on longitudinal aerodynamic characteristics is shown in Fig. 7. The

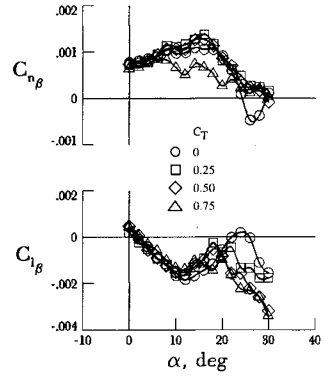

Fig. 13 Effect of power on lateral-directional stability, modified configuration.

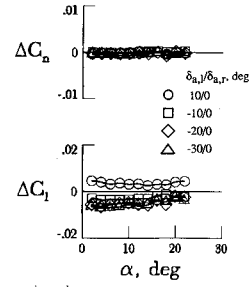

Fig. 14 Effect of aileron deflection on the baseline configuration.

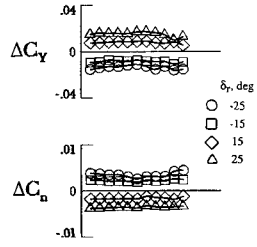

Fig. 15 Effect of rudder deflection on the baseline configuration.

data indicate that the leading-edge droop produced a flatter lift curve at the stall. Although the effect of the leading-edge droop was small on the overall lift characteristics, its effect on the flow over the outboard portion of the wing was found to be significant as indicated by the improved deep stall characteristics experienced in flight tests.

The effect of power on longitudinal aerodynamics characteristics of the modified Exdrone RPV is shown in Fig. 8. The thrust coefficients tested, C_T = 0.25, 0.50, and 0.75, represent power conditions up to maximum thrust at stall conditions. As expected, power effects increased the lift curve slope and maximum lift of the configuration. In addition, power effects decreased the longitudinal stability in the low-to-moderate angle-of-attack range. The decrease in longitudinal stability was caused by the incremental moment generated from the propeller normal force and the propeller slipstream interaction with the wing with increasing angle of attack, and was expected.

The effect of power on longitudinal trim is shown in Fig. 9 for the modified Exdrone configuration with the elevator set at the maximum deflection of 18 deg trailing-edge up. A comparison of the data of Figs. 8 and 9 indicate that the slipstream of the propeller increased the dynamic pressure over the elevator control surface, which resulted in the expected increased pitch control authority. From the power-off condition to the maximum thrust setting (C_T = 0.75), the maximum trimmed angle of attack increased from about 14 deg to about 21 deg, and the maximum trimmed lift coefficient increased from about 0.6 to 1.25.

Lateral-directional characteristics are shown in Figs. 10–19. Figure 10 shows the lateral-directional stability characteristics of the baseline configuration in the form of the stability derivatives $C_{n\beta}$ and $C_{l\beta}$. The data show that the baseline configuration exhibited stable dihedral effect, but low values of directional stability. The data also show that a vertical canard (see Fig. 1), which was placed on the baseline configuration to increase directional control, significantly degraded the directional stability of the baseline configuration. The value of $C_{n\beta}$ approached zero at an angle of attack of about 12 deg.

Several modifications were incorporated to improve directional stability (see Fig. 2). These modifications included increasing the rudder area, adding ventral tail area, moving the vertical tail 6 in. aft, and adding wingtip fins. A comparison of the lateral-directional stability characteristics of the baseline and the modified Exdrone configurations is presented in Fig. 11. The data indicate that the modifications more than doubled the directional stability $C_{n\beta}$ of the baseline configuration without significantly affecting the dihedral effect $-C_{l\beta}$ in the normal operating angle-of-attack range.

The contributions of various configuration components to the lateral-directional stability characteristics of the modified configuration are shown in Fig. 12. The configuration without the vertical tail was neutrally stable in yaw and became unstable near the stall onset (α = 12–16 deg). The addition of the vertical tail provided directional stability through the stall angle of attack; however, the directional stability became unstable above α = 24 deg. This yaw instability was probably caused by large vortical flow at high angles of attack, which at sideslip causes an adverse sidewash flowfield at the vertical tail (see Ref. 7). Addition of the wingtip fins provided a significant increment of directional stability at low-to-moderate angles of attack. Since the tip fin area was added mostly to the lower surface, the effective dihedral was not increased. At angles of attack above 20 deg, the configuration exhibited unstable values of $C_{l\beta}$. The addition of the wingtip fin and the leading-edge droop reduced the level of instability at the higher angles of attack.

The effects of power on the lateral-directional stability characteristics of the modified configuration are shown in Fig. 13. Without power, the configuration exhibited unstable dihedral effects at test angles of attack of α = 20–24 deg and unstable

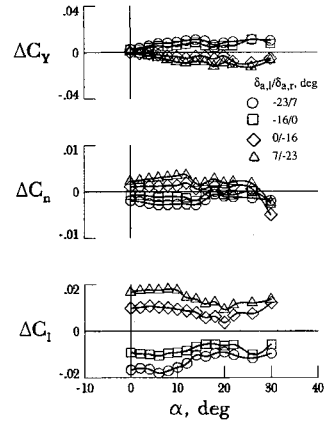

Fig. 16 Effect of aileron deflection on the modified configuration.

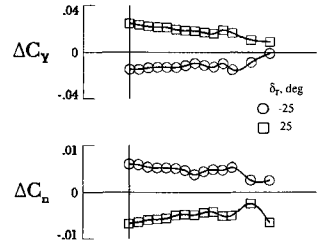

Fig. 17 Effect of rudder deflection on the modified configuration.

directional stability at test angles of attack of $\alpha = 22$–26 deg. With power on, the configuration exhibited stable lateral-directional stability throughout the test angle-of-attack range and a significant increase in lateral-direction stability at the higher test angles of attack. The increase in the stability of the configuration due to power effects at high angles of attack was probably caused by improvements in dynamic pressure and flowfield conditions from the interaction of the propeller slipstream on the vertical tail. At the maximum thrust setting ($C_T = 0.75$), the configuration exhibited stable but decreased values of directional stability at low-to-moderate angles of attack. This decrease in directional stability at the high power setting is likely associated with the amount of side force generated by the tractor propeller in sideslip conditions, which apparently offsets the increase in directional stability due to the improved flow on the vertical tail.

Lateral-directional control characteristics of the baseline configuration for $C_T = 0$ are shown in Figs. 14 and 15 for aileron and rudder control deflections, respectively. The aileron controls of the baseline configuration were set up for equal but opposite deflections. Aileron control power of the baseline configuration is shown in Fig. 14 for several deflection settings for only the left aileron control surface. The data show that the aileron control effectiveness was nonlinear. The configuration with ailerons set at $\delta_{a,l}/\delta_{a,r} = -30/0$ deg showed about as much incremental rolling moment ΔC_l as the configuration with $\delta_{a,l}/\delta_{a,r} = -20/0$ deg of deflection. Aileron control power remained relatively constant throughout the test angle-of-attack range. The data of Fig. 15 indicate that the rudder control authority of the configuration was relatively constant throughout the angle-of-attack range.

Lateral-directional control characteristics of the modified configuration at $C_T = 0$ are shown in Figs. 16 and 17 for aileron and rudder control deflections, respectively. For a maximum total differential aileron deflection of 30 deg, a comparison of the data of Figs. 14 and 16 indicate that the modified configuration exhibited an increase of maximum roll control over the baseline configuration. In addition, the aileron controls of the modified configuration with an offset in up travel provided more favorable yaw characteristics. The effect of the rudder on the modified configuration is shown in Fig. 17. Since the directional stability of the modified configuration was significantly increased, modifications were also made to increase rudder control power. The desired increase in rudder control power was accomplished by adding rudder area and moment arm. The data show that these modifications provided about 50% more rudder control authority than that of the baseline configuration. The data also show that the rudder consol authority was not significantly reduced at angles of attack up to 22 deg.

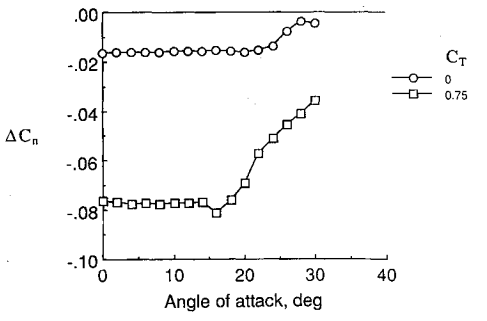

Fig. 18 Effect of power on rudder control authority of the modified configuration.

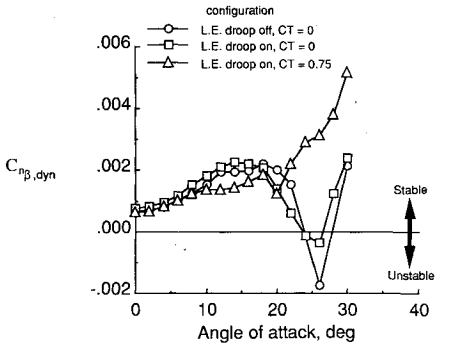

Fig. 19 Effect of leading-edge droop and power on the yaw divergence parameter, $C_{n\beta,\mathrm{dyn}}$, modified configuration.

The effects of power on the rudder control authority shown by the data of Fig. 18 indicate that the effects of power are quite large on the rudder control authority of this configuration. At low angles of attack, the yawing moment due to power with the maximum rudder deflection was about four times that of the power-off configuration. At angles of attack above 20 deg, there was a reduction in the yaw control authority; however, yaw control was still significantly greater with power on than with power off.

A plot of the dynamic directional stability parameter $C_{n\beta,\mathrm{dyn}}$ for the configuration with the leading-edge droop off and on is presented in Fig. 19. The data are generally in good agreement with the flight-test results and show that, with power on, the leading-edge droop had very stable values of $C_{n\beta,\mathrm{dyn}}$ at high angles of attack. No static tests were made with power on for the configuration with the leading-edge droop off.

Flight-Test Results

Qualitative flight-test evaluations were conducted only on the modified Exdrone RPV configuration. Flight tests of the modified configuration were initially conducted on a lightly loaded configuration of 45-lb gross weight at takeoff. During the test program, the weight of the vehicle was eventually increased beyond the design maximum takeoff gross weight of 65–70.5 lb. Flight-test maneuvers included the high-angle-of-attack and doublet flight maneuvers described earlier in the flight-test description section. The high-angle-of-attack maneuvers were assessed with and without the leading-edge droop modification.

The longitudinal stability and control characteristics of the modified Exdrone configuration were rated as very satisfactory by the test pilots over the nominal operating range of flight conditions tested. The modified vehicle exhibited stable short-period damping characteristics with the pitch motions completely damped within one cycle of oscillation. At higher wing loadings, the configuration was less responsive to controls, but was less sensitive to wind gusts. The vehicle without the leading-edge droop modification was controllable with full back stick and with the throttle set to idle power. However, with full power inputs, the maximum achievable angle of attack for the configuration without the leading-edge droop modification was limited by a lateral-directional stall departure despite corrective controls. With the leading-edge droop modification installed, no uncontrollable stall departures occurred for all conditions tested. The leading-edge droop modification did not change the pitch trim flight characteristics in the normal operating range of flight.

The lateral-directional flight characteristics of the modified Exdrone RPV configuration were considered to be very good in the low-to-moderate angle-of-attack range. With the small chord ailerons, the vehicle roll response was considered to be slow, whereas with the larger chord ailerons of the modified configuration, the vehicle was considered satisfactory in roll response. With the roll rate gyro turned on, the vehicle's lateral responsiveness, as expected, was reduced, but overall lateral-directional flying qualities were greatly improved.

At high angles of attack, with test conditions of full back-stick input and at idle power, the configuration without the leading-edge droop modification was marginally controllable in flight and required constant attention to roll and yaw control inputs to prevent a lateral-directional stall departure. With power on, the configuration without the leading-edge droop exhibited a roll departure against full corrective con-

trol. This departure characteristic was observed on the configuration with the roll rate gyro turned either on or off.

With the leading-edge droop installed, the lateral-directional flight characteristics of the vehicle were significantly improved at high angles of attack. The addition of the leading-edge droop greatly reduced the roll-off tendency at high angles of attack. This improvement was likely due to increased roll damping. Previous investigations of various general aviation configurations in wind-tunnel dynamic force tests have confirmed that roll damping is generally increased with the use of the outboard leading-edge droop modification at high angles of attack.

Summary of Results

At the request of the United States Marine Corps, an exploratory wind-tunnel and flight test investigation was conducted by NASA Langley Research Center to improve the stability, controllability, and general flight characteristics of the Marine Corps Exdrone RPV configuration. The investigation included exploratory wind-tunnel static tests and radio-controlled flight tests.

The wind-tunnel static tests identified several deficiencies in the longitudinal and lateral-directional stability and control characteristics of the baseline configuration, which led to several modifications for improved stability and control characteristics. The configuration modifications that proved to be most effective included increased elevator area, increased vertical tail area and moment arm, increased rudder area and aileron area, the addition of vertical wingtip fins, and the addition of a leading-edge droop to the outboard wing panel.

The results of the radio-controlled flight tests showed that the modified configuration had good longitudinal and lateral-directional flight characteristics over the test angle-of-attack range. The configuration was very maneuverable and responsive to control inputs, exhibited good damping characteristics, and was easily flyable through the stall with no departure tendencies.

References

[1]Ross, H. M., Yip, L. P., Perkins, J. N., Vess, R. J., and Owens, D. B., "Wing Leading-Edge Droop/Slot Modification for Stall Departure Resistance," *Journal of Aircraft*, Vol. 28, No. 7, 1991, pp. 436–442.

[2]"Exploratory Study of the Effects of Wing-Leading-Edge Modifications on the Stall/Spin Behavior of a Light General Aviation Airplane," NASA TP 1589, Dec. 1979.

[3]Yip, L. P., King, P. M., Muchmore, C. B., and Davis, P., "Exploratory Wind Tunnel Investigations of the Low-Speed Stability and Control Characteristics of Advanced General Aviation Configurations," AIAA Paper 86-2596, Oct. 1986.

[4]Yip, L. P., Robelen, D. B., and Meyer, H. F., "Radio-Controlled Model Flight Tests of a Spin Resistant Trainer Configuration," AIAA Paper 88–2146, May 1988.

[5]Johnson, J. L., Jr., Yip, L. P., and Jordan, F. L., Jr., "Preliminary Aerodynamic Design Considerations for Advanced Laminar Flow Aircraft Configurations," NASA CP 2413, 1986, pp. 185–226.

[6]Fratello, D. J., Croom, M. A., Nguyen, L. T., and Domack, C. S., "Use of the Updated NASA Langley Radio-Controlled Drop-Model Technique for High-Alpha Studies of the X-29A Configuration," AIAA Paper 87-2559, Aug. 1987.

[7]Chambers, J. R., and Anglin, E. L., "Analysis of Lateral-Directional Stability Characteristics of a Twin-Jet Fighter Airplane at High Angles of Attack," NASA TN D-5361, Aug. 1969.